Monaldi Archives for Chest Disease

eISSN 2532-5264 https://www.monaldi-archives.org/

Monaldi Arch Chest Dis 2024 [Online ahead of print]

To cite this Article:
Pozza A, Avesani M, Cattapan I, et al. **Multimodality imaging and functional assessment in patients with systemic right ventricle and biventricular physiology: a retrospective single-center study.** *Monaldi Arch Chest Dis* doi: 10.4081/monaldi.2024.3085

Multimodality imaging and functional assessment in patients with systemic right ventricle and biventricular physiology: a retrospective single-center study

Alice Pozza,[1*] Martina Avesani,[1*] Irene Cattapan,[1] Elena Reffo,[1] Annachiara Cavaliere,[2] Jolanda Sabatino,[1,3] Sofia Piana,[1] Anna Molinaroli,[1] Domenico Sirico,[1] Biagio Castaldi,[1] Alessia Cerutti,[1] Roberta Biffanti,[1] Giovanni di Salvo[1]

[1]Pediatric Cardiology Unit, Department of Women's and Children's Health, University of Padua; [2]Pediatric Radiology, Neuroradiology Unit, University Hospital of Padua; [3]Pediatric Cardiology Unit, Magna Graecia University, Catanzaro, Italy

[*]These authors contributed equally to this work and share the first authorship

Correspondence: Martina Avesani, Pediatric Cardiology Unit, Department of Women's and Children's Health, University of Padua, Via Giustiniani, 2 35128 Padua, Italy.
Tel.: 0498211400. E-mail: martina.avesani@aopd.veneto.it.

Contributions: AP, reviewed the literature, drafted and edited the work; MA, JS, revised the work critically; MA, IC, worked on statistical analysis; ER, AC, analyzed cardiac magnetic resonance imaging; SP, AM, AC, RB, BC, DS, collected clinical data; GDS, proposed the topic, designed the work, and reviewed the final version.

Conflict of interest: the authors declare no conflict of interest.

Ethics approval and consent to participate: institutional review board approval was not required for this study as only de-identified compliant data were used in the analysis.

Patient consent for publication: not applicable.

Funding: this research received no external fundings.

Availability of data and materials: data and materials are available from the corresponding author.

Abstract

Systemic right ventricle (sRV) dysfunction is frequent in patients with congenitally corrected transposition of great arteries (cc-TGA) and those with dextro-transposition of great arteries (D-TGA) after Mustard/Senning operations. This condition should be identified promptly. We aimed to compare echocardiographic parameters with cardiac magnetic resonance (CMR)-derived parameters in patients with sRV and to evaluate their correlation with clinical variables and exercise capacity.

Patients with cc-TGA and D-TGA after Mustard/Senning who underwent standard and advanced (speckle tracking and 3D) echocardiography and CMR (including feature-speckle tracking) were included. Clinical and imaging parameters were collected. Echocardiographic-derived right ventricle end-diastolic area and end-systolic area correlated with 3D echocardiographic-derived right ventricle end-diastolic and end-systolic volume (r=0.6, p=0.006 and r=0.8, p=0.002). 3D ejection fraction (EF) correlated with fractional area change and tricuspid annular plane systolic excursion (TAPSE) (r=0.8, p=0.001 and r=0.7, p=0.03). sRV global longitudinal strain correlated with systemic atrial strain (sAS) (r=-0.6, p=0.01). CMR-derived EF correlated with CMR-derived global longitudinal strain (GLS) both endocardial and myocardial (r=-0.7, p=0.007 and r=-0.6, p=0.005). sRV areas as assessed by echo correlated with CMR-derived volumes (r=0.9, p=0.0001 for diastole and r=0.8, p=0.0001 for systole). Similarly, a correlation was found between sRV echo-derived GLS and CMR-derived GLS, both endocardial and myocardial (r=0.8, p=0.001 and r=0.7, p=0.01). The only imaging parameter which correlated with peak V02 was sAS (r=0.55, p=0.04). When comparing cc-TGA and D-TGA, the former showed better GLS-derived values as assessed by CMR (CMR-derived right ventricle endocardial longitudinal strain -23.2% *versus* -17.2%, p=0.002; CMR-derived right ventricle myocardial longitudinal strain -21.2% *versus* -16.7%; p=0.05), bigger systemic atrial area (20.2 cm^2/m^2 *versus* 8.4 cm^2/m^2, p=0.005) and higher TAPSE values (16.2 mm *versus* 12.2 mm, p=0.04).

Echocardiography is valid to screen for sRV dilatation and function and to guide the timing for CMR. The investigation of atrial deformation imaging may help to better understand diastolic function. Patients with cc-TGA show better cardiac function compared to patients after atrial switch. Further investigations are needed to identify imaging parameters linked to exercise capacity.

Key words: systemic right ventricle, cardiac magnetic resonance imaging, cardiopulmonary exercise test, echocardiography.

Abbreviations:

sRV: systemic right ventricle
CHDs: congenital heart diseases
cc-TGA: congenitally corrected transposition of the great arteries
D-TGA: dextro transposition of great arteries
CMR: cardiac magnetic resonance
CPET: cardiopulmonary exercise testing
eRV-EDA: echo-derived right ventricle end-diastolic area
eRV-ESA: echo-derived right ventricle end-systolic area
eRV-EDAi: indexed echo-derived right ventricle end-diastolic area
eRV-ESAi: indexed echo-derived right ventricle end-systolic area
eESA_sA: echo-derived systemic atrium end-systolic area
eESA_sAi: indexed echo-derived systemic atrium end-systolic area
FAC: fractional area change
TAPSE: tricuspid annular plane systolic excursion
RV-GLS: right ventricle global longitudinal strain
sA: systemic atrium
sAS: systemic atrium peak systolic strain
eRV-EDV: echo-derived right ventricle end-diastolic volume
eRV-ESV: echo-derived right ventricle end-systolic volume
eRV-EDVi: indexed echo-derived right ventricle end-diastolic volume
eRV-ESVi: indexed echo-derived right ventricle end-systolic volume
eRV-EF: echo-derived right ventricle ejection fraction
cRV-EDV: CMR-derived right ventricle end-diastolic volume
cRV-ESV: CMR-derived right ventricle end-systolic volume
cRV-EDVi: indexed CMR-derived right ventricle end-diastolic volume
cRV-ESVi: indexed CMR-derived right ventricle end-systolic volume
cRV-EF: CMR-derived right ventricle ejection fraction
cRV-GLSendo: CMR-derived right ventricle endocardial longitudinal strain
cRV-GLSmyo: CMR-derived right ventricle myocardial longitudinal strain

Introduction

The systemic right ventricle (sRV) condition, where the morphological right ventricle supports systemic circulation, accounts for approximately 10% to 12% of all congenital heart diseases (CHDs) [1,2]. This unique anatomical and functional adaptation occurs in both two-ventricle and single-ventricle arrangements, presenting a spectrum of clinical phenotypes and prognoses. Biventricular physiologies involving sRV are typically seen in patients with congenitally corrected transposition of the great arteries (cc-TGA) and those with dextro-transposition of the great arteries (D-TGA) who have undergone Mustard or Senning operations. While many of these patients survive into adulthood, they often face progressive sRV dysfunction, heart failure, exercise intolerance, arrhythmias, and premature death in early adulthood [3-7]. sRV failure is a significant concern for congenital heart disease practitioners, necessitating longitudinal follow-up to identify markers of cardiac dysfunction and implement appropriate treatments. A recent consensus paper has provided comprehensive guidelines and recommendations for the effective use of integrative imaging technologies in CHDs, with special insights on sRV [8]. Echocardiography remains the first-line diagnostic technique, yet its application is challenging due to the lack of specific cut-off values and quantitative parameters tailored to sRV. Additionally, obtaining optimal acoustic windows in these patients can be difficult [9]. Cardiac Magnetic Resonance (CMR) offers a more reliable quantitative assessment of sRV function but is limited by longer execution times, higher costs, and limited availability [10,11]. Currently, multimodality imaging with integration of different methodologies allows to overcome challenges of sRV, thus improving management and long-term prognoses of affected patients [12].

This study aims to: i) compare a comprehensive range of standard and advanced echocardiographic parameters with CMR-derived parameters in patients with sRV and biventricular physiology (D-TGA post-Mustard/Senning operations and cc-TGA); ii) evaluate their correlation with clinical variables and exercise capacity.

Materials and Methods

Study population

This is a retrospective single center study, carried out at the Department for Women's and Children's Health of Padua University Hospital between March and September 2023.

Patients were included if they met the following criteria:

- sRV and biventricular circulation in D-TGA with previous Mustard or Senning surgery or cc-TGA
- patients were considered eligible for this study if they had an echocardiogram and a CMR scan within one year from last follow-up visit (September 2022-September 2023).

Patients excluded from the study were those implanted with pacemaker, cardioverter defibrillator or any CMR incompatible device.

Patients' records were reviewed from the medical platform of Padua University Hospital. Clinical data extracted from medical record included: age, body mass index, body surface area (BSA), New York Heart Association (NYHA) functional class, time since surgery and ongoing medications. Moreover, data derived from cardiopulmonary exercise test (CPET) done within 12 months from any imaging exam were collected, when available. The following parameters were considered: peak oxygen consumption (VO_2 peak), minute ventilation/carbon dioxide production (VE/VCO_2) slope, metabolic equivalents (METs) and peak respiratory exchange ratio (RER). All data was collected keeping confidentiality and was anonymized for statistical analysis.

Cardiac resting imaging

All the echo studies were performed by using Vivid E95 ultrasound system (General Electric Healthcare, Horten, Norway). Standard and advanced transthoracic echocardiographic exams were performed by one experienced pediatric cardiologist (MA).

Chamber quantification measurements were assessed according to the current European Association of Echocardiography guideline [13]. From the apical window we measured: RV end-diastolic and end-systolic area (eRV-EDA, eRV-ESA), and atrial end-systolic area (eESA_sA). These values were then normalized for BSA.

Global sRV function was visually assessed from the apical four chamber view. Fractional area change (FAC) was calculated as the percentage of change between the eRV-EDA and eRV-ESA. Tricuspid annular plane systolic excursion (TAPSE) was determined in M-MODE. Tricuspid inflow PW Doppler velocities, lateral wall TDI velocities and the derived E/E' ratio were also assessed.

Speckle tracking global longitudinal strain (GLS) of sRV, including RV free wall and septum (eRV-GLS), was calculated in the apical four chamber view on the ultrasound device itself or on an offline workstation (Echo PAC version 112.99, Research Release, GE Healthcare), which allows semi-automated analysis.

The images selected for the speckle tracking analysis had a frame rate between 50 and 100 frames per second, with a 10% variability in heart rate, as already detailed in previous articles on speckle tracking echocardiography and congenital heart diseases [14,15]. After having drawn manually 3 points (2 annular and 1 apical), the software tracked the myocardium semi-automatically throughout the heart cycle. Manual adjustments, if needed, were performed to optimize the region of interest. The automated algorithm allowed global longitudinal strain to be calculated, dividing the right ventricles in 6 segments. GLS by speckle tracking was defined as the average peak negative value on the strain curve during the systole. Segments not well visualized were not included, in case of two non-visualizable segments the patient was not included in the analysis.

From the apical four chamber view, the systemic atrium (sA) peak systolic strain was also measured (sAS). The atrial wall was traced manually (3 points) and adjusted, if necessary, resulting in strain curves from a total of 3 atrial segments. Global peak atrial strain was defined as the average of the maximum positive values during RV systole of the 3 analyzed atrial segments.

When available, 3D images were elaborated to obtain 3D volumes (eRV-EDV, eRV-ESV) and ejection fraction (eRV-EF).

Tricuspid regurgitation was evaluated as none/trivial (0 = single narrow jet), mild (1 = multiple narrow jets), moderate (2 = wide jet reaching the mid part of the atrium) and severe (3 = wide jet reaching the roof of the atrium). The color scale was set at a Nyquist limit of 50–60 cm/s. Analysis of echocardiographic data was blind to CMR results, clinical data, and CPET findings.

Each CMR examination was carried out by one pediatric cardiologist experienced in pediatric CMR imaging (ER) and one pediatric radiologist (AC) with the same CMR scanner (Achieva 1.5 Tesla, Philips Healthcare; Best, the Netherlands). CMR measurements were performed by the same operator (ER), to empower data consistency and assessment was blind to Echo data.

A standard CMR protocol for evaluating patients with sRV includes: real-time localization imaging in three planes without ECG-gating and during free breathing; cine SSFP sequence with gated-breathing to report anatomy, size of ventricles and function; phase contrast (PC) sequences Qp:Qs; whole-heart isotropic 3D SSFP imaging for vascular evaluation without contrast material administration and visualization of proximal and mid-coronary arteries; LGE imaging along the long and the short axes [16].

In the following study, we evaluated steady-state free precession (SSFP) end-inspiratory breath-hold ECG-gated cine-images in long axis views and a stack of short-axis slices covering the ventricular cavities. Moreover, right ventricular outflow tract (RVOT) obstruction was assessed by specific RVOT view, together with analysis of the superior systemic venous pathways and possible presence of baffle leaks.

All patients underwent Gadolinium 0.2 mmol/kg administration to assess the presence of late gadolinium enhancement (LGE) in the 4-chamber and short-axis view.

Image analysis was performed by using Philips Intellispace Cardiovascular post-processing software. The sRV epi- and endocardium were manually segmented in cine short axis on end-diastolic and end- systolic images. The following data were considered: sRV volumes both absolute and indexed to BSA (cRV-EDV, cRV-ESV) and EF (cRV-EF) [17,18].

Myocardial strain was assessed using feature tracking (FT) applied to SSFP cine images during post-processing with a dedicated software (Qstrain, Medis Suite Version 4.0.38.4, Leiden, Netherlands). Global longitudinal strain of the sRV (cRV-GLSendo, cRV-GLSmyo) was evaluated on long-axis images [17,18]. Initially, the endocardial borders of the sRV were manually segmented in the end-diastolic phase and then automatically expanded to all phases with an automatic border detection algorithm. The endocardial borders were checked for accuracy in all cardiac phases and manually adjusted if necessary. The software provided endocardial and myocardial peak systolic strain [19,20]. Finally, we compared Echo and CMR data with values measured by CPET.

Statistical analysis

Baseline characteristics are reported as percentages for categorical variables, as means and standard deviations for continuous variables when normality was verified, and as median and interquartile range (IQR) when normality was not verified by the Kolmogorov–Smirnov test. The Student's t-test for independent samples or the Mann–Whitney test when normality was not verified was used for the analysis of the variables. Differences between groups for continuous variables were analyzed based on distribution using t-test, Kruskal-Wallis test or Wilcoxon-Mann-Whitney test, as appropriate.

The relationship between CMR-derived data, echocardiographic parameters and exercise test results was evaluated using the Pearson and Spearman correlation coefficient as appropriate.

The statistical significance was set at p-value <0.05. Analysis was performed using SPSS statistic software version 22 (IBM SPSS Statistics Version 22, Chicago IL, USA).

Results

Patients

Twenty-two patients with sRV and biventricular physiology underwent echocardiography and CMR between September 2022 and September 2023. Both echocardiographic and CMR data were available for 19 patients. Median age at CMR was 28 years (IQR 17,25-33); 11 (58%) were female. Eleven patients had cc-TGA, 4 of them had previous physiologic repair, consisting of large ventricle septum defect closure (3 patients) and atrial septal defect closure (1 patient). Of the 8 patients with D-TGA 5 had undergone Senning repair (63%). cc-TGA patients were significantly younger than patients with D-TGA (p 0.03; cc-TGA median age 21 years IQR 16,25-28,5; D-TGA median age 32 years IQR 28,25-36,75). Most patients were clinically asymptomatic. Demographic and clinical features of patients are summarized in Table 1.

Cardiac imaging

Echocardiographic and CMR data were available in 19 patients. 2D speckle tracking echocardiography was available in 15 patients, 3D echocardiography in 11 patients, CMR feature tracking was assessed in 18 performed scans. TR was assessed as mild in 4 patients (21%), moderate in 13(68.4%) and severe in 2 (10.5%) patients. Echocardiographic and CMR variables are summarized in Table 2.

Echocardiographic results

A correlation between eRV-EDA and eRV-EDV and between eRV-ESA and eRV-ESV, both as absolute (rho 0.6, p 0.006; rho 0.8, p 0.002) and indexed values (rho 0.8 p 0.007; rho 0.9 p 0.0001) was found. In addition, a correlation between eRV-EF and FAC and TAPSE was identified (r 0.8, p 0.001 and r 0.7, p 0.03). Also, E/E′ correlated inversely with sAS (r -0.8, p 0.03). Lastly, the correlation between sAS and RV-GLS was also statistically significant (r -0.6, p 0.01). No correlation was found between other echocardiographic data and NYHA class.

CMR results

A correlation was found between cRV-EF and CMR-GLS, both endocardial and myocardial (r -0.7, p 0.007, r -0.6, p 0.005). No correlation was found between CMR-derived data and myocardial fibrosis or NYHA class.

Echo and CMR results

A statistically significant correlation was found between cRV-EDV and cRV-ESV and eRV-EDA and ESA (r 0.9, p 0.0001; r 0.8, p 0.0001 respectively). Also, cRV-GLSendo and cRV-GLSmyo correlated significantly with RV-GLS assessed by echocardiography (r 0.8, p 0.001; r 0.7, p 0.01 respectively) and cRV-GLSendo correlated with sAS (r -0.6, p 0.04). These results are shown in Figure 1. No correlation was found between CMR-derived data and other echocardiographic parameters.

CPET and cardiac imaging

CPET was available for 17 patients. No correlation was found between CMR imaging parameters and CPET functional data. This result did not change even when evaluating cc-TGA and TGA Mustard/Senning patients separately. The only echocardiographic parameter that correlated with peak V02 was sAS (r 0.55, p 0.04).

cc-TGA and TGA-Mustard/Senning

When cc-TGA and D-TGA patients were compared, the former showed better GLS values as assessed by CMR (cRV-GLSendo -23.2% vs -17.2%, p 0.002; cRV-GLSmyo -21.2% vs -16.7%; p 0.05); and bigger indexed systemic atrial area (20.2 cm^2/m^2 vs 8.4 cm^2/m^2, p 0.005). TAPSE values were higher in cc-TGA group (16.2 mm vs 12.2 mm, p 0.04). Also, a trend was noticed towards worse values of sAS in D-TGA (13.8% vs 21.0%, SD 7.6 and 6.9 respectively). These results are shown in Figure 2.

No differences were noticed in terms of tricuspid regurgitation and peak VO2 between the two populations (D-TGA 22.2 ml/kg/min; ccTGA 25.8 ml/kg/min).

Discussion

To the best of our knowledge, only a few studies compared standard and advanced echocardiographic parameters with CMR parameters and CPET in patients with sRV and biventricular physiologies, sometimes even yielding conflicting results [21].

This study contributes to the limited body of research comparing standard and advanced echocardiographic parameters with CMR parameters and CPET in patients with sRV and biventricular physiologies. Our findings confirm that echocardiography is a well established clinical tool for the clinical follow up of these patients, to evaluate sRV dilatation and to assess systolic function . Also, further investigations of diastolic function in these patients, particularly by assessing atrial strain, may help in better understating the role of diastole in exercise capacity. Lasty, our findings suggest that some differences in terms of cardiac function exists in patients with sRV and different cardiac anatomies.

In this study, a significant correlation was found between 2D echo-derived areas and CMR-derived volumes confirming that 2D echocardiography is a valid first tool to screen right ventricular dilatation, to assess patients longitudinally and to guide the timing for advanced imaging such as CMR. Indeed, CMR remains a solid tool to assess sRV, but high costs, lower availability and the need for dedicated skilled staff may limit its use [11].

Three-dimensional echocardiography is an advanced imaging technique that could provide a wealth of information for the evaluation of sRV. Nevertheless, the semi-automated software for 3D analysis needs good quality images, sometimes difficult to achieve when evaluating sRV in TGA population [22]. Some studies reported a correlation between echo volumes and CMR volumes [23,24]. This was not identified in our study, but the small sample size may have limited the analysis. Indeed, considering that sRV areas by echocardiography correlated significantly with 3D volumes, we can speculate that with a bigger sample size we might have reached the same result also in comparison with CMR data.

Previous studies demonstrated a good correlation between strain measurements obtained by echocardiography and CMR, and data from our study supports this finding [10,25]. Also, in this study, a significant correlation was found between sAS and RV-GLS assessed by echo. Impaired atrial function, as it can be in patients after Mustard/Senning operations, can lead to inadequate ventricular filling [26,27]. This may affect firstly ventricular diastolic function and, later, systolic performance. This can potentially lead to decreased cardiac output and, ultimately, heart failure. Thus, monitoring both atrial and ventricular strain parameters longitudinally could provide valuable insights to early identify patients at risk for adverse outcomes and guide treatment strategies [28]. In addition, the systematic assessment of atrial strain may help to better understand diastolic function in these patients, which is still poorly understood [29-31].

The correlation between sAS and peak VO2 may suggest a major role of diastolic function in determining exercise capacity in patients with sRV. The relationship between atrial deformation imaging and peak VO2 has been already investigated in other CHDs [32,33]. By contrast, previous echocardiographic and CMR studies investigated the correlation between functional imaging parameters and CPET in patients with sRV, with no significant results [23,26]. However, atrial deformation imaging was not performed in these studies. Based on the results of the current study we speculate that the presence of pulmonary veins baffle and tricuspid regurgitation can alter atrial compliance and elasticity, especially under exercise, resulting in an insufficient atrial output into sRV. Lastly, compared to subjects with D-TGA, patients with cc-TGA showed better systolic function, as assessed by CMR-derived GLS values, higher values of TAPSE, systemic atrial area, and a trend toward better values of sAS. These results might be partially explained by the degree of TR, which leads to atrial enlargement and enhance TAPSE values [34,35]. However, in our study we did not find a difference when comparing the degree of TR among the two subgroups, thus other mechanisms such as altered ventriculo-atrial coupling and issues about atrial contraction may be involved. Ultimately, the absence of atrial surgery could explain the trend toward higher sAS values in cc-TGA group.

Limitations

We acknowledge certain limitations of our study. This is a retrospective, single institution cohort study, thus advanced imaging was not available for all patients. Furthermore, some correlation coefficients are based on a small sample size as measurements were not feasible/available in a considerable number of cases. However, this reflects practical applicability in everyday clinical practice, as echocardiographic assessment of sRV function is challenging and patients with sRV represent a rare populatio.

Conclusions

The study reaffirms the value of echocardiography as a primary tool for assessing sRV dimensions and function and guiding the timing for CMR use. The better systolic performance in cc-TGA patients compared to those with D-TGA reflects the distinct characteristics and natural history of these conditions. Lastly, the use of 3D echocardiography and the assessment of diastolic function in this population remain areas that need further development.

References

1. Ho SY, Nihoyannopoulos P. Anatomy, echocardiography, and normal right ventricular dimensions. Heart 2006;92:i2-13.

2. Foschi M, Di Mauro M, Tancredi F, et al. The dark side of the moon: the right ventricle. J Cardiovasc Dev Dis 2017;4:18.

3. Morrison ML, Grant B, McCrossan BA, et al. 32 year follow up of patients following atrial redirection surgery for transposition of the great arteries. Congenit Heart Dis 2019;14:846-53.

4. Gelatt M, Hamilton RM, McCrindle BW, et al. Arrhythmia and mortality after the Mustard procedure: a 30-year single-center experience. J Am Coll Cardiol 1997;29:194-201.

5. Lebherz C, Gerhardus M, Lammers AE, et al. Late outcome, therapy and systemic ventricular function in patients with a systemic right ventricle: data of the German National Register for Congenital Heart Defects. Cardiol Young 2022;32:1235-45.

6. Ciuca C, Balducci A, Angeli E, et al. Long term follow-up of patients with systemic right ventricle and biventricular physiology: a single centre experience. J Cardiovasc Dev Dis 2023;10:219.

7. Brida M, Diller G-P, Gatzoulis MA. Systemic Right ventricle in adults with congenital heart disease: anatomic and phenotypic spectrum and current approach to management. Circulation 2018;137:508-18.

8. Festa P, Lovato L, Bianco F, et al. Recommendations for cardiovascular magnetic resonance and computed tomography in congenital heart disease: a consensus paper from the CMR/CCT working group of the Italian Society of Pediatric Cardiology and the Italian College of Cardiac Radiology endorsed by the Italian Society of Medical and Interventional Radiology (part II). J Cardiovasc Med 2024;25:473-87.

9. Iriart X, Horovitz A, Van Geldorp IE, et al. The role of echocardiography in the assessment of right ventricular systolic function in patients with transposition of the great arteries and atrial redirection. Arch Cardiovasc Dis 2012;105:432-41.

10. Obokata M, Nagata Y, Wu VC-C, et al. Direct comparison of cardiac magnetic resonance feature tracking and 2D/3D echocardiography speckle tracking for evaluation of global left ventricular strain. Eur Heart J Cardiovasc Imaging 2016;17:525-32.

11. Samyn MM, Yan K, Masterson C, et al. Echocardiography vs cardiac magnetic resonance imaging assessment of the systemic right ventricle for patients with d-transposition of the great arteries status post atrial switch. Congenit Heart Dis 2019;14:1138-48.

12. Moscatelli S, Avesani M, Borrelli N, et al. Complete transposition of the great arteries in the pediatric field: a multimodality imaging approach. Children 2024;11:626.

13. Lang RM, Badano LP, Mor-Avi V, et al. Recommendations for cardiac chamber quantification by echocardiography in adults: an update from the American Society of

Echocardiography and the European Association of Cardiovascular Imaging. J Am Soc Echocardiogr 2015;28:1-39.e14.
14. Sabatino J, Di Salvo G, Krupickova S, et al. Left ventricular twist mechanics to identify left ventricular noncompaction in childhood. Circ Cardiovasc Imaging 2019;12:e007805.
15. Prota C, Di Salvo G, Sabatino J, et al. Prognostic value of echocardiographic parameters in pediatric patients with Ebstein's anomaly. Int J Cardiol 2019;278:76-83.
16. Fratz S, Chung T, Greil GF, et al. Guidelines and protocols for cardiovascular magnetic resonance in children and adults with congenital heart disease: SCMR expert consensus group on congenital heart disease. J Cardiovasc Magn Reson 2013;15:51.
17. Gregov A, Hrabak Paar M. Magnetic resonance imaging assessment of right ventricular deformation in patients with transposition of the great arteries. J Thorac Imaging 2022;37:W85-91.
18. Morais P, Marchi A, Bogaert JA, et al. Cardiovascular magnetic resonance myocardial feature tracking using a non-rigid, elastic image registration algorithm: assessment of variability in a real-life clinical setting. J Cardiovasc Magn Reson 2016;19:24.
19. Rajiah PS, Kalisz K, Broncano J, et al. Myocardial strain evaluation with cardiovascular mri: physics, principles, and clinical applications. RadioGraphics 2022;42:968-90.
20. Scatteia A, Baritussio A, Bucciarelli-Ducci C. Strain imaging using cardiac magnetic resonance. Heart Fail Rev 2017;22:465-76.
21. Helsen F, De Meester P, Van De Bruaene A, et al. Right ventricular systolic dysfunction at rest is not related to decreased exercise capacity in patients with a systemic right ventricle. Int J Cardiol 2018;260:66-71.
22. Molnár AÁ, Sánta A, Merkely B. Echocardiography imaging of the right ventricle: focus on three-dimensional echocardiography. Diagnostics 2023;13:2470.
23. Kutty S, Li L, Polak A, et al. Echocardiographic knowledge-based reconstruction for quantification of the systemic right ventricle in young adults with repaired D-transposition of great arteries. Am J Cardiol 2012;109:881-8.
24. Schneider M, Beichl M, Nietsche C, et al. Systematic evaluation of systemic right ventricular function. J Clin Med 2019;9:107.
25. Claus P, Omar AMS, Pedrizzetti G, et al. tissue tracking technology for assessing cardiac mechanics. JACC Cardiovasc Imaging 2015;8:1444-60.
26. Franzoso FD, Wohlmuth C, Greutmann M, et al. Atrial function after the atrial switch operation for transposition of the great arteries: comparison with arterial switch and normals by cardiovascular magnetic resonance. Congenit Heart Dis 2016;11:426-36.
27. Gaynor SL, Maniar HS, Prasad SM, et al. Reservoir and conduit function of right atrium: impact on right ventricular filling and cardiac output. Am J Physiol Heart Circ Physiol

2005;288:H2140-5.
28. Dorobantu DM, Amir NH, Wadey CA, et al. The role of speckle-tracking echocardiography in predicting mortality and morbidity in patients with congenital heart disease: a systematic review and meta-analysis. J Am Soc Echocardiogr 2024;37:216-25.
29. Gaynor SL, Maniar HS, Bloch JB, et al. Right atrial and ventricular adaptation to chronic right ventricular pressure overload. Circulation 2005;112:I212-8.
30. Ta HT, Alsaied T, Steele JM, et al. Atrial function and its role in the non-invasive evaluation of diastolic function in congenital heart disease. Pediatr Cardiol 2020;41:654-68.
31. Avesani M, Borrelli N, Krupickova S, et al. Echocardiography and cardiac magnetic resonance in children with repaired tetralogy of Fallot: new insights in cardiac mechanics and exercise capacity. Int J Cardiol 2020;321:144-9.
32. Rato J, Mendes SC, Sousa A, et al. The Influence of atrial strain on functional capacity in patients with the fontan circulation. Pediatr Cardiol 2020;41:1730-8.
33. Silini A, Avesani M, Houyel L, et al. The pivotal role of tricuspid regurgitation in the failing systemic right ventricle: the "chicken and egg story". Arch Cardiovasc Dis 2022;115:476-86.
34. Muraru D, Badano LP, Hahn RT, et al. Atrial secondary tricuspid regurgitation: pathophysiology, definition, diagnosis, and treatment. Eur Heart J 2024;45:895-911.
35. Marelli AJ, Ionescu-Ittu R, Mackie AS, et al. Lifetime prevalence of congenital heart disease in the general population from 2000 to 2010. Circulation 2014;130:749-56.

Table 1. Demographic and clinical features of the study cohort. Values are expressed as mean + standard deviation, median (interquartile range), or n (%).

Variables	Study cohort (n=19)
Age at CMR	28 (IQR 17,25-33)
cc-TGA age (years)	21 (IQR 16,25-28,5)
D-TGA age (years)	32 (IQR 28,25-36,75)
Female	11 (58%)
cc-TGA, (%)	11 (57,9%)
D-TGA, (%) s/p Mustard s/p Senning	8 (42,1%) 3 (37%) 5 (63%)
NYHA class II, n (%)	(7,36,8 %)
Ongoing treatment (%) Beta-blocker ACE-I Diuretics Anticoagulants Antiaggregant Sacubitril/valsartan	 4 (21%) 4 (21%) 2 (10.5%) 2 (10.5%) 1 (5.2%), 2 (10.5%)
Peak VO2 (ml/kg/min)	24.3 (SD 6.6)
VE/VCO2	32.6 (SD 3.9)
Peak RER	1.16 (SD 0.1)
METS	12.8 (SD 2.4)

SD, standard deviation; CMR, cardiac magnetic resonance; cc-TGA, congenitally corrected transposition of the great arteries; D-TGA, dextro transposition of great arteries; NYHA, New York Heart Association; peak VO2, peak oxygen consumption; VE, minute ventilation; VCO2, carbon dioxide production; peak RER, peak respiratory exchange ratio; METs, metabolic equivalent of task.

Table 2. Cardiac magnetic resonance and echo variables analyzed in the study. Values are mean + standard deviation or n (%).

Echocardiographic variables	**Study cohort (n=19)**
eRV-EDA (cm^2)	31,06 (SD 9,14)
eRV-EDAi (cm^2/m^2)	22,48 (SD 12,38)
eRV-ESA (cm^2)	20,13 (SD 8,61)
eRV-ESAi (cm^2/m^2)	14,24 (SD 8,34)
FAC (%)	37,41 (SD 7,62)
E/A	2 (SD 1,03)
TAPSE (mm)	13,93 (SD 5,24)
S'velocity (cm/s)	9,55 (SD 2,66)
E/E'	12,04 (SD 6,09)
E' velocity (m/s)	0,96 (SD 0,28)
eRV-EDV (ml)	127,18 (SD 40,67)
eRV-EDVi (ml/m^2)	81,32 (SD 32,51)
eRV-ESV (ml)	67,26 (SD 29,55)
eRV-ESVi (ml/m^2)	42,52 (SD 20,15)
eRV-EF (%)	47,44 (SD 8,88)
eRV-GLS (%)	-15,35 (SD 4,02)
eESA_sA (cm^2)	21,50 (SD 12,13)
eESA_sAi (cm^2/m^2)	15,35 (SD 9,87)
sAS (%)	18,17 (SD 7,87)
Moderate-severe TR, n (%)	15 (78%)
CMR variables	**Study cohort (n=19)**
cRV-EDV (ml)	170.25 (SD 73.56)
cRV-EDVi (ml/m^2)	104.61 (SD 22.79)
cRV-ESV (ml)	87.22 (SD 39.94)
cRV-ESVi (ml/m^2)	67,72 (SD 61,15)
cRV-EF (%)	50,11 (SD 8,44)
FAC (%)	34.16 (SD 10.45)
cRV-GLSendo	-20.62 (SD 5.35)
cRV-GLSmyo	-19.22 (SD 4.99)

SD, standard deviation; eRV, echo-derived right ventricle; cRV, CMR-derived right ventricle; EDA, end-diastolic area; ESA, end-systolic area; EDAi, indexed end-diastolic area; ESAi, indexed end-systolic area; FAC, fractional area change; TAPSE, tricuspid annular plane systolic excursion; EDV, end-diastolic volume; ESV, end-systolic volume; EDVi, indexed end-diastolic volume; ESVi, indexed end-systolic volume; EF, ejection fraction; GLS, global longitudinal strain; sA, systemic atrium; sAi, indexed systemic atrium; sAS, systemic atrium peak systolic strain; TR, tricuspid regurgitation.

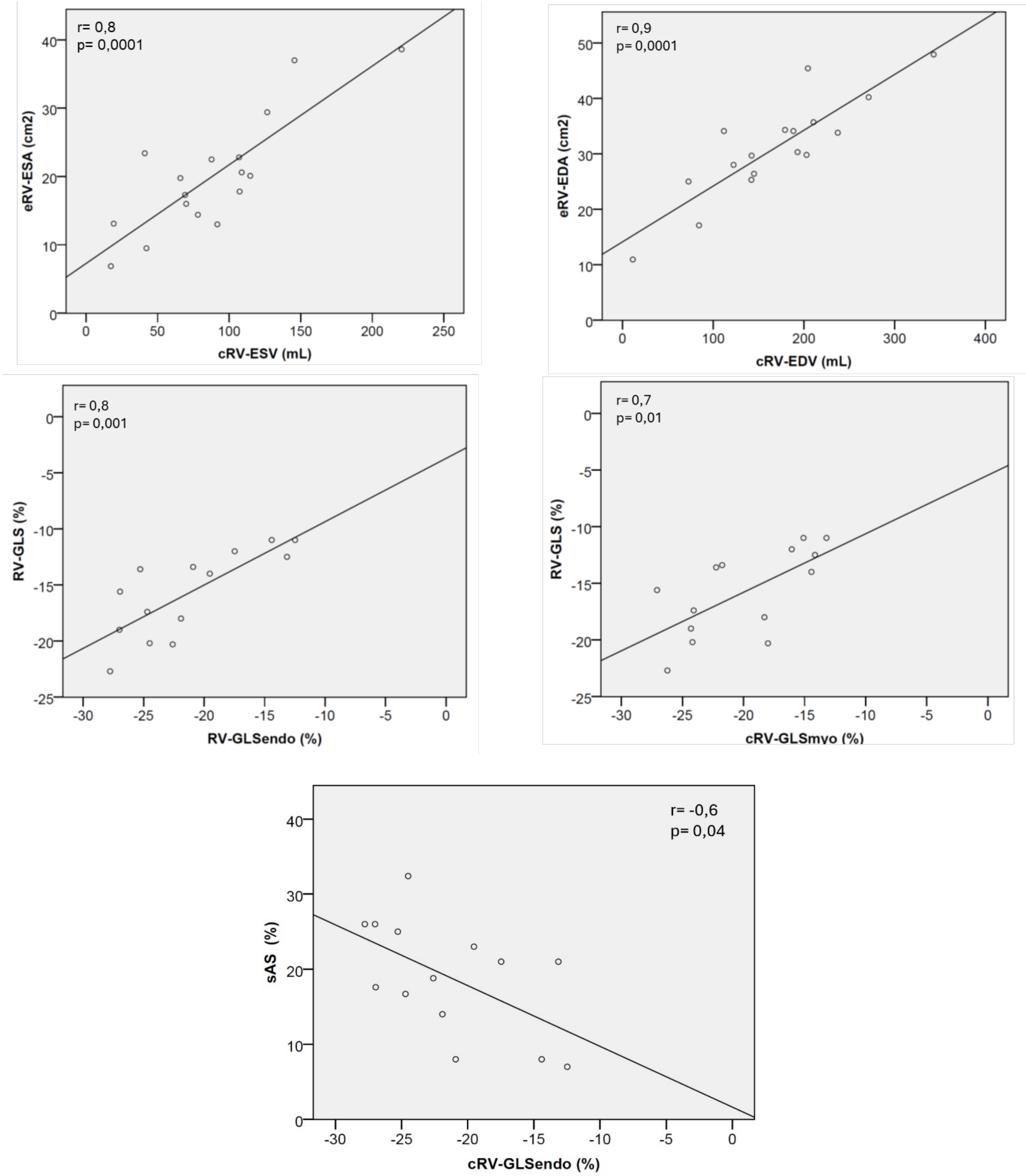

Figure 1. Scatterplot showing the correlation between CMR-and Echo derived parameters. eRV-ESA, echo-derived right ventricle end-systolic area; cRV-ESV, CMR-derived right ventricle end-systolic volume; eRV-EDA, echo-derived right ventricle end-diastolic area; cRV-EDV, CMR-derived right ventricle end-diastolic volume; RV-GLS, right ventricle global longitudinal strain; cRV-GLSendo, CMR-derived right ventricle endocardial longitudinal strain; cRV-GLSmyo, CMR-derived right ventricle myocardial longitudinal strain, sAS: systemic atrium peak systolic strain.

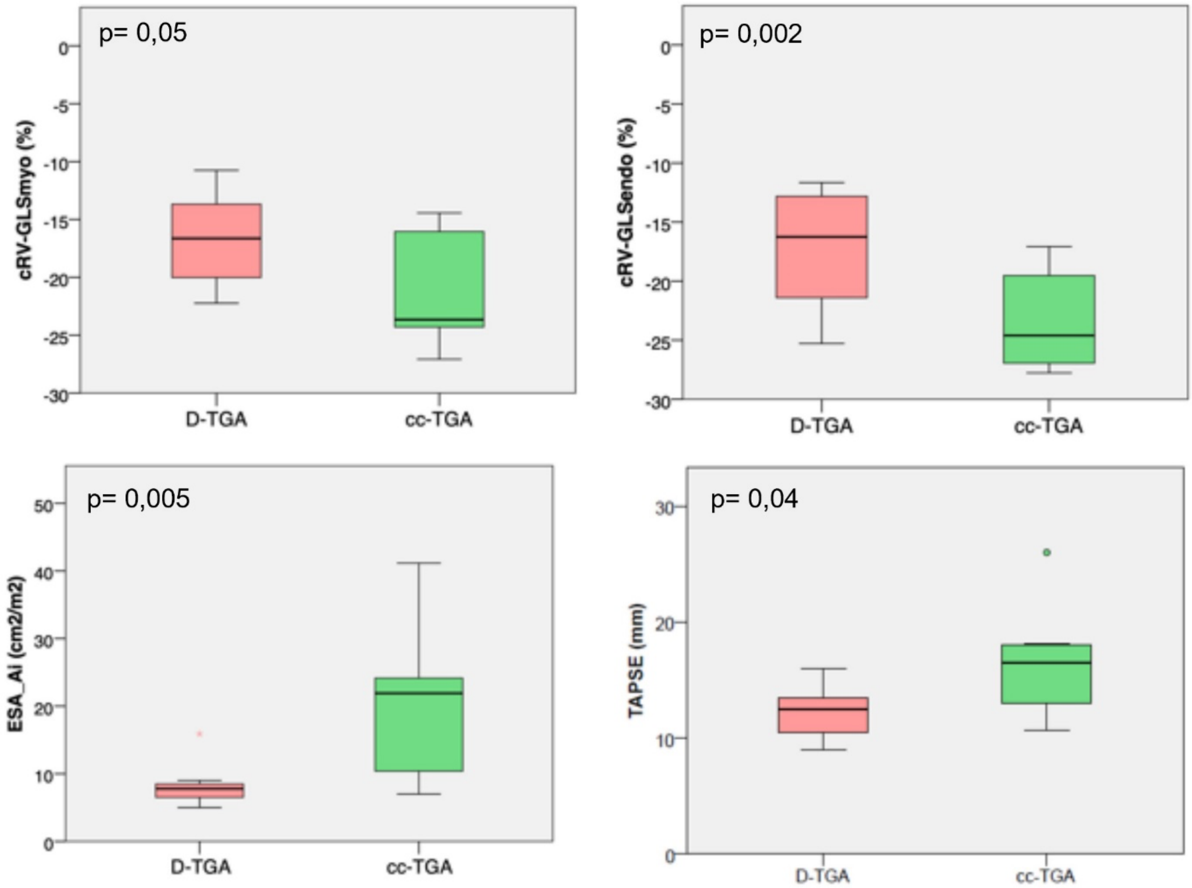

Figure 2. Distribution of GLS, ESA_Ai and TAPSE in the two TGA subgroups. cRV-GLSmyo, CMR-derived right ventricle myocardial longitudinal strain; cRV-GLSendo, CMR-derived right ventricle endocardial longitudinal strain; ESA_Ai, indexed echo-derived systemic atrium end-systolic area; TAPSE, tricuspid annular plane systolic excursion.